Theoretical assessment on the possibility of constraining point-defect energetics by pseudo phase transition pressures

Hua Y. Geng, Hong X. Song, and Q. Wu

National Key Laboratory of Shock Wave and Detonation Physics, Institute of Fluid Physics, CAEP, P.O. Box 919-102 Mianyang, Sichuan 621900, People's Republic of China

(Received 10 January 2013; published 20 May 2013)

Making use of the energetics and equations of state of defective uranium dioxide that are calculated with first-principles methods, we demonstrate the possibility of constraining the formation energy of point defects by measuring the transition pressures of the corresponding pseudo phase of defects. The mechanically stable range of fluorite structure of UO_2, which dictates the maximum possible pressure of relevant pseudo phase transitions, gives rise to defect formation energies that span a wide band and overlap with the existing experimental estimates. We reveal that the knowledge about pseudo phase boundaries can not only provide important information on energetics that is helpful for reducing the scattering in current estimates, but also be valuable for guiding theoretical assessments, even to validate or disprove a theory. In order to take defect interactions into account and to extrapolate the physical quantities at finite stoichiometry deviations to that near the stoichiometry, we develop a general formalism to describe the thermodynamics of a defective system. We also show that it is possible to include interactions among defects in a simple expression of a point defect model (PDM) by introducing an auxiliary constant mean field. This generalization of the simple PDM leads to great versatility that allows one to study nonlinear effects of stoichiometry deviation on materials' behavior. It is a powerful tool to extract the defect energetics from finite defect concentrations to the dilute limit. Besides these, the full content of the theoretical formalism and some relevant and interesting issues, including reentrant pseudo transition, multiple-defect coexistence, charged defects, and possible consequence of instantaneous defective response in a quantum crystal, are explored and discussed.

DOI: 10.1103/PhysRevB.87.174107 PACS number(s): 64.60.Bd, 61.72.J−, 64.30.Jk, 62.50.−p

I. INTRODUCTION

Defects usually play a prominent role in various properties of a solid. For this reason, the physics and chemistry of defects have been the subjects of much study for several decades.[1] Many of these works focused mainly on the dilute limit, i.e., with a small defect concentration. This is the case of interest in doped semiconductors and/or compounds in the immediate vicinity of the stoichiometry. At certain conditions (usually with high temperature) deviation from the stoichiometry can span over a wide range of chemical composition. Binary oxides CeO_2 and UO_2 represent the paradigms for such kind of nonstoichiometry in the fluorite-related structures, and many others exist as well.[2] For a comprehensive understanding of these materials, knowledge from just near the stoichiometry is insufficient. This is because many physical quantities depend strongly on nonstoichiometry, and exhibit quite different behavior when at finite deviations. On the other hand, defects at high pressure have received little attention so far, and our knowledge about their general behavior at highly compressional conditions is very limited, in spite of the fact that they are crucial for Earth modeling and for planetary evolution description, where plenty of defects present a variety of nonstoichiometric minerals in the interior of these celestial bodies. The capability to capture correctly the energetics and other physical properties across the whole stoichiometry range at different temperature-pressure conditions is an essential requirement for the purpose of predicting and controlling the behavior of these complex materials. Nevertheless, a general theoretical method for this purpose is still elusive.

Even at ambient conditions and near the stoichiometry, our understanding about nuclear oxides such as UO_2 and $(U,Pu)O_2$ is also limited and unsatisfactory.[2] Although there are many papers and reports that have been published on various aspects of diffusion in these oxides, a reasonable level of understanding has been reached only in the case of oxygen, from which the formation energy of the oxygen Frenkel pair can be deduced when the migration energy of the corresponding diffusion process is known.[2–6] Nevertheless, measuring oxygen diffusion in stoichiometric oxides is difficult because of the need to maintain the stoichiometry, which is almost impossible for a large temperature range.[3] The difficulty also lies in the interpretation of available experimental data. While theoretical calculations can be applied to individual processes, transport and other data often correspond to a superposition of several entangled processes and make extraction of the desired information complicated.[4–6] In addition to chemical diffusion and self-diffusion, electrical conductivity[5] and neutron scattering[7] have also been performed to measure the defect concentrations and formation energies. In all of these experiments, a poor understanding of the experimental conditions, as well as the inherent difficulties in the measurement and subsequent interpretation of data, has caused dispersed results.[3,6,8]

There are also very few experimental data existing for cation defects in nuclear oxides.[3] For example in UO_2, only crude estimates of the activation energy for uranium self-diffusion and migration energy of uranium vacancy are available. With the aid of a point defect model (PDM), one can extract the Schottky defect formation energy from these estimates. But since a great uncertainty remains in the experimental data, the reliability of the derived value is doubtful.[8]

Progress in density functional theory of electrons and in computational algorithms make it possible to calculate the

relevant energetics directly from quantum mechanics. Such kind of first-principles methods have provided better data than previous semiempirical interatomic potentials, and are comparable to experimental measurements. The electronic structures,[9–11] structural phase transformations[12,13] and equations of state (EOS),[13–15] oxygen diffusion,[16–18] and some defect clustering structures[18–22] have been modeled. Unfortunately, this advance has never reached a satisfactory level for defect energetics, even though much effort has been devoted to it.[8,19,20,23–32] It cannot even reproduce the experimental fact that oxygen defects dominate the whole stoichiometry range.[8,20] Also one should note that including oxygen clusters can give rise to the expected predominance of oxygen defects,[14,21,22] but its relevance to the experimentally measured defect formation energy is unclear.[32] This discrepancy among experimental and theoretical results might be due to the limited accuracy of the theoretical assessments, for example the possible metastable electronic states that could be encountered in calculations of strongly correlated materials,[33–36] the approximation employed to treat the partially localized 5*f* orbitals,[37–41] the variation of the charge state of defects,[29–32] and the small size of the simulation cell for defective structure modeling that is currently accessible. All of these might render uncertain error in the final results. But this also can arise from the error lying in the experimental estimates that are widely used as the benchmark for theoretical modeling: The data are scattered and not fully self-consistent, and in some cases these estimated data cannot reproduce the fact of the predominance of oxygen defects, too.[3,6,8] This makes the problem entangled and very hard to treat. Therefore any approach that can constrain the defect energetics and reduce its uncertainty is of decisive help for solving the problem.

In this report, we investigate the possibility of a such kind of method by examining the physics that governs the pressure-driven pseudo transitions[15] between different defect species. By establishing a theoretical relationship of the pseudo phase boundary on defect formation energies, we show that strict constraints can be imposed on these energy parameters, which might then be used to refine the experimental estimates. To achieve the final goal, however, one has first to measure the curve of pseudo transition pressures and obtain accurate equations of state of defects, and then make use of the theoretical method that we will present below, to get reliable estimate of defect formation energies. In this sense this report is the first step—but also the most important step—towards this accomplishment. By developing the theoretical basis of this constraining procedure, it not only provides us a new angle to understand the long-standing problem, but also establishes a general method in treating highly defective materials under high pressures. For the clarity of discussion, we will first present a simple theoretical framework using PDM that is intuitive and easy to understand, and then a generalization to the general case will be made.

In Sec. II we discuss the PDM that allows us to calculate the pseudo phase diagram of point defects, and then establish a relationship between pseudo phase boundary and defect energetics. Using this powerful tool, the influence of intrinsic defect formation energy on pseudo transition is then investigated in Sec. III. The obtained information represents a constraint on the possible value of the formation energy of the defects. Though our discussion is mainly focused on uranium dioxide in this paper, we also extend the investigation by considering virtual models to explore other interesting phenomena such as reentrant pseudo transition and multiple-defect coexistence, in Sec. III B. It is well known that PDM does not take defect-defect interactions into account and can be applied to only the vicinity of the stoichiometry. In order to deal with highly defective regions and extrapolate the energetic and thermodynamic information obtained at finite stoichiometry deviations to the dilute limit, a general formalism that can treat defect interactions is developed in Sec. IV. This generalization is necessary for a realistic description of the nonlinear dependence of thermodynamic properties on nonstoichiometry. A brief discussion and remarks on charge state of defects, as well as other relevant issues, are then given in Sec. V, which is followed by a summary of the main conclusions.

II. SIMPLE THEORETICAL FRAMEWORK

At dilute limits where defect concentration is negligibly small, imperfectness in crystal has little impact on thermodynamic and mechanical properties, despite a profound modification on electrical conductivity and/or magnetism that might often occur. At large stoichiometry deviation, the defect concentration is governed by the ratio of chemical compositions rather than by thermal excitation; therefore the density of defects could be enormous. In this case, noticeable influence on general thermodynamic quantities can be expected, so as on relevant mechanical properties.

To understand the general effects of nonstoichiometry on a material's behavior, we require a physical model that expresses the defect density as a function of external conditions—usually the hydrostatic pressure and temperature—and how the presentation of defects modifies thermodynamic functions such as enthalpy or Gibbs free energy. Having such a function that incorporates defect effects, all relevant thermodynamic properties can be derived straightforwardly. In this section we first present the basic picture by considering the simple PDM. A general formalism will be developed in Sec. IV.

In the PDM,[3,42] the spatial size of an individual defect is assumed to be of zero dimension, and all interactions among them are neglected. In this simple model, defect concentrations are determined by the corresponding formation energy of isolated defects. Considering a structure that contains one defect of type i, its Gibbs free energy can be written as

$$G_i(P,T) = E_c(V) + F_{\rm ph}(V,T) + PV, \tag{1}$$

in which P, T, and V stand for hydrostatic pressure, temperature, and volume of the simulation cell, respectively. The cohesive energy at zero kelvins in static approximation reads

$$E_c(V) = -D + \frac{9}{8}B_0V_0\left[\left(\frac{V_0}{V}\right)^{2/3} - 1\right]^2 \tag{2}$$

when expressed in Birch-Murnaghan equation (other EOS models can be used as well). Here variables with subscript 0 denote the corresponding value in the equilibrium condition of zero pressure, and B is the bulk modulus. The contribution of lattice dynamics to the free energy can be approximated in

the Debye model as

$$F_{\rm ph}(V,T) = 3k_BT\ln[1-\exp(-\Theta_D/T)] - k_BTf(\Theta_D/T) + \tfrac{9}{8}k_B\Theta_D, \quad (3)$$

where k_B is the Boltzmann constant and f the Debye function. The Debye temperature can be evaluated approximately by[43,44]

$$\Theta_D = \Theta_D^p\left[\frac{BM^p}{B^pM}\left(\frac{v}{v^p}\right)^{1/3}\right]^{1/2}. \quad (4)$$

Here the superscript p denotes the reference state (here the defect-free UO_2), v is the effective volume per atom, and M is the effective atomic weight. The parameters in these equations, namely D, B_0, and V_0, can be obtained by fitting to *ab initio* results of density functional theory, while Θ_D^p can be taken from x-ray diffraction measurement.[45,46] The details of determining the value of these parameters have been discussed and presented in Ref. 14.

Having known G_i, the formation Gibbs free energy (FGE) of intrinsic point defects can be constructed. For example, the FGE of a Frenkel pair (FP) of species X is then expressed as

$$\Delta G_{\rm X\_FP} = G_{X_v}^{N-1} + G_{X_i}^{N+1} - 2G^N, \quad (5)$$

and for the Schottky defect (S) as (taking UO_2 as the example)

$$\Delta G_{\rm S} = G_{\rm U_v}^{N-1} + 2G_{\rm O_v}^{N-1} - 3\frac{N-1}{N}G^N. \quad (6)$$

Here N denotes the number of atoms in a defect-free cell and G^N is the corresponding Gibbs free energy; $G_{X_v,X_i}^{N\pm1}$ is the Gibbs free energy of the cell containing the respective defect. In a closed regime where no particle exchange with the exterior can occur, the defect concentration must satisfy[8,14,20]

$$[V_{\rm O}][I_{\rm O}] = \exp\left(\frac{-\Delta G_{\rm O\_FP}}{k_BT}\right), \quad (7)$$

$$[V_{\rm U}][I_{\rm U}] = \exp\left(\frac{-\Delta G_{\rm U\_FP}}{k_BT}\right), \quad (8)$$

$$[V_{\rm O}]^2[V_{\rm U}] = \exp\left(\frac{-\Delta G_{\rm S}}{k_BT}\right). \quad (9)$$

The composition equation that expressed in point defect populations is

$$x = \frac{2([V_{\rm U}]-[I_{\rm U}])+[I_{\rm O}]-2[V_{\rm O}]}{1-[V_{\rm U}]+[I_{\rm U}]}, \quad (10)$$

where x is the stoichiometry deviation (for example that in UO_{2+x}). Notice that Eq. (10) is different from the conventional definition of

$$x = 2([V_{\rm U}]-[I_{\rm U}])+[I_{\rm O}]-2[V_{\rm O}], \quad (11)$$

which is valid only when no cation defect is involved. We thus complete the formalism of the PDM, in which the defect concentrations are determined by solving Eqs. (7)–(10).

Since no interaction among defects has been taken into account in the PDM, the total Gibbs free energy of a defective system is a linear superposition of the contribution of each individual defect. That is,

$$G \approx G_0 + \sum_i \frac{\Delta G_i}{n_i^{\rm ref}}n_i, \quad (12)$$

where G_0 is the Gibbs free energy of the defect-free matrix. The defect concentration n_i runs over $[I_{\rm O}]$, $[V_{\rm O}]$, $[I_{\rm U}]$, and $[V_{\rm U}]$, respectively, with the superscript "ref" indicating the corresponding value in a defective reference system, and $\Delta G_i = G_i^{\rm ref} - G_0$. From Eq. (12) thermodynamic quantities as a function of stoichiometry deviation x can be derived.

III. PSEUDO PHASE DIAGRAM AND PSEUDO TRANSITION

In defective crystals, distinction of the physics mainly originates from the predominant defect species. Thanks to the exponential dependence of defect concentrations on the formation energy, most regions in the phase space spanned by temperature, pressure, and chemical composition (T-P-x) are dominated by only one type of defect. One can then use the concept of pseudo phase to simplify the description of defective (nonstoichiometric) materials.[15] In this picture, each pseudo phase corresponds to a region that is governed by a homogeneous distribution of a *single* type of defect. Here no effects of migration and creation or annihilation of defects are considered, which is justified if we focus mainly on the *long-time averaged* properties only.

With variation of the thermodynamic conditions of T, P, and x, the predominant defect might change from one type into another; i.e., pseudo phase transition (PPT) might take place. Physical quantities that are affected by defects also change rapidly along this transition.[15] From this perspective, the physics of defects can be greatly simplified to that of each individual pseudo phases and their respective behavior at the PPT. It is thus important to understand the extent of the control region of each pseudo phase, namely, the pseudo phase diagram (PPD). From Eqs. (7)–(10), it is evident that such a diagram is completely described by the energetics of each defect. Conversely, if we know the PPD, then constraints on defect formation energies can be established.

It is natural to define the transition point of a PPT as where defect concentration increases/decreases to half of its saturate value; then the corresponding pseudo phase boundary (for example in UO_{2+x}) is determined by

$$\frac{1}{2x} = \exp\left(\frac{-\Delta G_{\rm S} + 2\Delta G_{\rm O\_FP}}{k_BT}\right) \quad (13)$$

for a transition between U_v and O_i when $x > 0$, and

$$-\frac{2}{x} = \exp\left(\frac{\Delta G_{\rm S} - \Delta G_{\rm U\_FP}}{k_BT}\right) \quad (14)$$

between U_i and O_v when $x < 0$ (only point defects are considered). Because all ΔG are functions of T and P (and also depend on x via defect interactions, which we discarded here but will discuss in detail below), solutions of Eq. (13) and (14) provide a set of constraints on formation energy of intrinsic defects.

A. Realistic system: UO_2

This subsection is devoted to a realistic system of UO_2, where involved parameters are obtained by density functional theory calculations. Since early experiments were driven by application of UO_2 as a nuclear fuel, most investigations

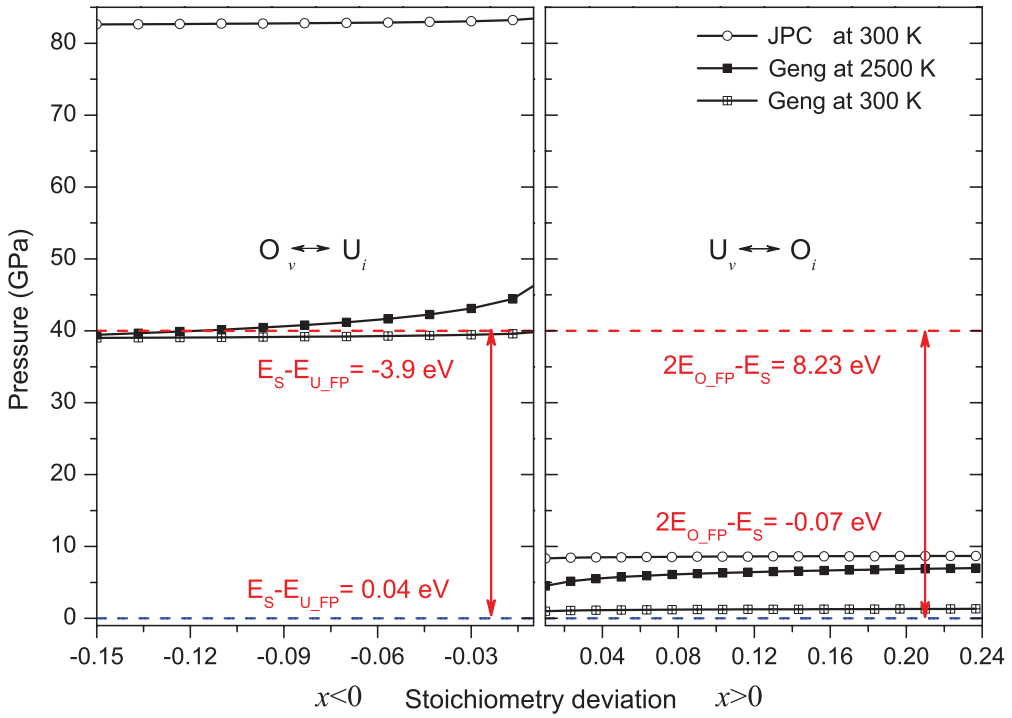

FIG. 1. (Color online) Comparison of the pseudo phase diagram of UO_{2+x} calculated with Crocombette (JPC; Ref. 32) and Geng's (Ref. 14) formation energies of defects. The constraints on intrinsic defect formation energies when the pseudo transition pressure is bounded between 0 and 40 GPa are also shown.

focused mainly on formation energy of intrinsic defects, which closely relates to the parameter D in Eq. (2). To be consistent with conventional notations, we use E_S, E_{O_FP}, and E_{U_FP} to denote the formation energy of Schottky defect, oxygen Frenkel pair, and uranium Frenkel pair at zero pressure and temperature, respectively. Based on the defect energetics calculated by Geng *et al.* for uranium dioxide,[14] the PPD on the P-x plane is evaluated and shown in Fig. 1. It can be seen that in the region of $x < 0$ an increase of temperature from 300 to 2500 K has little influence on the pseudo boundary. However, on the $x > 0$ side, such a size of change in T leads to an increase of the pseudo transition pressure about 5 GPa. Overall, the impact of x on the PPD at the PDM level of approximation is small, and with an opposite trend for the hypo- and hyperstoichiometry regions.

There are a few other theoretical assessments of the defect energetics for UO_2 available in the literature.[8,19,20,23–32] Unfortunately in most cases only formation energy at 0 GPa and 0 K were given, from which, however, one cannot determine the pseudo transition pressure because the information about the variation with temperature and pressure is lost. Under an assumption that the compression behavior and phonon contribution are the same for all of these calculations, which is a simple but reasonable approximation, we can estimate the corresponding pseudo transition boundary by adjusting the D in Eq. (2) accordingly to yield the respective formation energy at 0 GPa and 0 K using Geng's equation of state.[14] Here we choose the data of J. P. Crocombette (JPC) for the purpose of comparison, since they are typical ones that have considered possible charge states of defects, thus producing a formation energy of oxygen Frenkel pair and Schottky defect that seems in a good agreement with experimental estimates.[32] By adjusting D to reproduce the E_S and E_{O_FP} of JPC, we obtained the estimated PPD of JPC's data. Note here we have made an assumption that the charge state of each defect is fixed during compression or heating, and the formation energy of the uranium interstitial was taken from Geng's data because in JPC's work no value for this defect type was given.

The PPD calculated with JPC's formation energy is drawn in Fig. 1 for comparison. On the $x < 0$ side, the transition from O_v to U_i takes place at a much higher pressure. This is reasonable since JPC's data have a lower formation energy for O_v than Geng's evaluation, which gives rise to a stronger stability of this defect. On the $x > 0$ side, the uranium vacancy was predicted to be the predominant defect at low pressure, and the transition to O_i occurs at about 8 GPa. This result is consistent with previous PDM evaluations at zero hydrostatic pressure, where U_v was predicted to be the major defect component. Nevertheless, the prevailing U_v is contradictory to the experimental observation that the oxygen defect should dominate this region, indicating that the experimental estimate of the defect formation energy might be inconsistent in itself.[3,6,8] This difficulty could stem from the procedure of extraction defect energetics from diffusion measurements. Usually the employed physical models were very simple and might lead to inaccurate explanation of the measured data.[3–6]

On the other hand, as mentioned above, PPD provides valuable information about possible range of the defect formation energy. For UO_2, the PPT in fluorite structure (if exists) should be bounded between a pressure range of 0 and 40 GPa, because at higher pressures UO_2 transforms into the *Pnma* phase,[47] which is followed by an isostructural

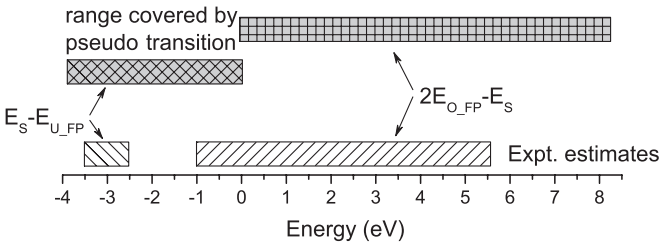

FIG. 2. A schematic diagram which illustrates the range of defect formation energy that is covered by pressure-driven pseudo transition (upper part) and the corresponding experimental estimates (lower part) in nonstoichiometric UO_2.

transition,[13] and finally converges to isotropic $P6_3/mmc$ structure[12] according to recent theoretical predictions. Under this restriction, the formation energy of intrinsic defects should satisfy

$$-3.9\ \text{eV} \leqslant E_S - E_{U\_FP} \leqslant 0.04\ \text{eV} \tag{15}$$

when $x < 0$, and

$$-0.07\ \text{eV} \leqslant 2E_{O\_FP} - E_S \leqslant 8.23\ \text{eV} \tag{16}$$

when $x > 0$ for a PPT to occur between a pressure of 0 and 40 GPa. These constraints are marked in Fig. 1 together with dashed lines that indicate the corresponding bounded range of pressure.

Theoretical assessment explicitly suggests that U_v definitely becomes unfavorable under compressional conditions. Therefore the experimental observation that O_i prevails in the $x > 0$ region implies that there should be no PPT from U_v to O_i at any pressures greater than zero. Then from Eq. (16) one gets

$$E_S \geqslant 2E_{O\_FP} + 0.07\ \text{eV}, \tag{17}$$

which puts a strong constraint on possible value of defect formation energies. For example the experimental estimates of E_{O_FP} lie in between 3.0–4.6 eV and E_S between 6.0–7.0 eV.[3,7] If we take E_S as 7.0 eV, then E_{O_FP} must be less than 3.5 eV. This value is, however, incompatible with the most reliable experimental assessments.[4,5,7] On the other hand, if we take the neutron scattering measurement[7] of 4.6 eV as a reliable estimate for E_{O_FP}, then E_S must be greater than 9.3 eV. This in turn disqualifies most theoretical estimates with charged defects.[29,32] In a word, all of these indicate that we need further scrutiny on these estimates, and any alternative and/or complemental information on defect energetics are decisive to reach the final conclusion. The inequalities of Eqs. (15) and (16) cover most ranges of the experimental estimates, as shown in Fig. 2. Thus they can provide new understanding about this issue if we can measure the compression-driven PPT of point defects experimentally.

B. Virtual system: Model study

Defective behavior of materials at high pressure is determined by the variation of defect formation enthalpy with compression. It is also affected by possible structural transitions of the matrix. The above discussion elaborated what might happen in a compressed nonstoichiometric UO_2. In other materials, however, much more complex phenomena can be expected. From a theoretical perspective, it is helpful to explore all possibilities in order to grasp the general feature of the physics of defects. In the simple PDM approximation, the physics is mainly determined by the parameters appeared in Eq. (2), i.e., the value of D, B_0, and V_0 of each defective configuration that were employed to derive the formation Gibbs free energy (FGE). Therefore we can arbitrarily alter these parameters to probe other interesting behaviors of defects that are allowed in theory but not in the realistic UO_2.

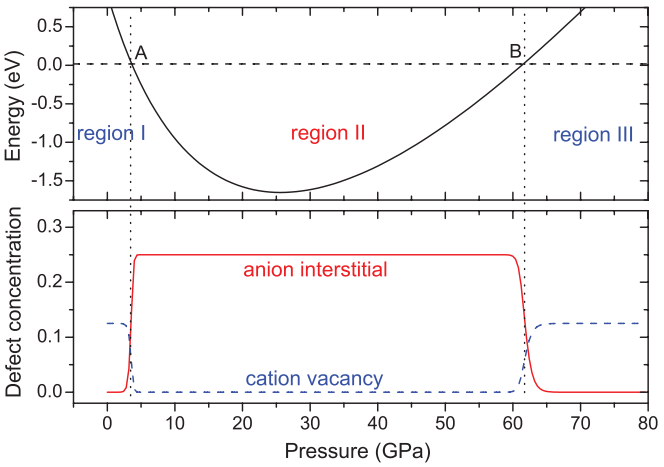

FIG. 3. (Color online) Pressure-driven reentrant pseudo transition of defects at 300 K and $x = 0.25$. Upper panel: Energy variation; lower panel: defect concentrations.

1. *Reentrant transition*

The first phenomenon we would like to discuss is reentrant transition. It is a rare type of phase change even for a conventional physical state, where one phase that has been transformed into another reappears. On the phase diagram the corresponding phase boundary is a reentrant curve. Analogous phenomenon can also take place in the PPT, where the predominant defect species first changes into another type, and then transforms back. The condition of this transition is completely governed by Eqs. (7)–(9). Put explicitly, if the derived equation [Eq. (13) or (14)] has multiple solutions, then the corresponding PPT is reentrant.

Figure 3 demonstrates a virtual dioxide compound that has a reentrant PPT. In the upper panel, a graphical solution of Eq. (13) is drawn where the solid line is the term of $-\Delta G_S + 2\Delta G_{O\_FP}$. Another term of $k_B T \ln(\frac{1}{2x})$ is also shown as a dashed line in the figure. The points of intersection A and B correspond to the solutions of Eq. (13), which also are the locations where the PPT takes place. In the lower panel, the change of defect concentrations along compression is illustrated, from which one can clearly see that cation vacancy reappears at higher pressures.

It is necessary to point out that this result was obtained by subtracting 145 GPa from the bulk modulus of all defective UO_2 configurations and thus might be an artifact. Nevertheless, such a virtual model can help us acquire a profound understanding of a material's behavior that has reentrant PPT, if it exists. The resultant modifications on the EOS and thermodynamic properties across this transition region are interesting. Figure 4 illustrates the compression

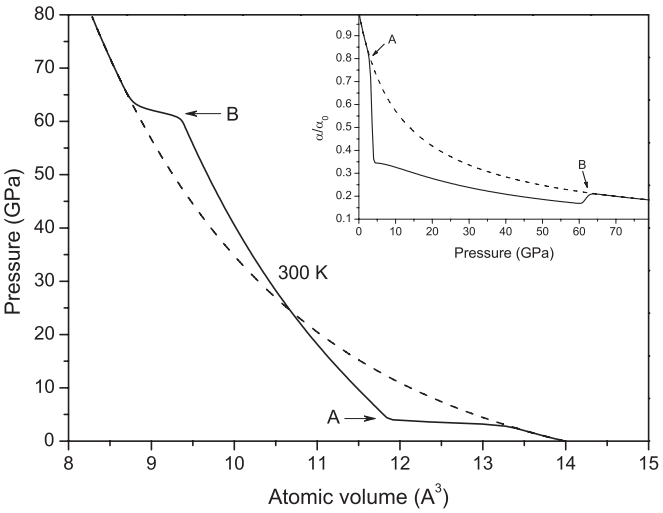

FIG. 4. Isothermal compression curve of a reentrant PPT as showing in Fig. 3. Inset: The relative variation of thermal expansivity.

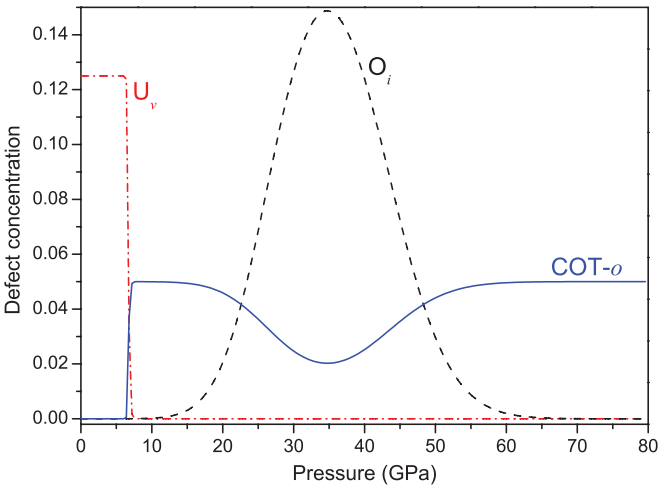

FIG. 5. (Color online) Multiple-defect coexistence at 300 K and $x = 0.25$; see text for details.

behavior of the same PPT as in Fig. 3, in which the restoring of the compression curve at the high pressure end is evident. There are two volume collapses in the reentrant PPT at points A and B, respectively. Between A and B, the curve is steeper. This is consistent with the requirement for a pressure-driven reentrant transition to occur; namely, the intermediate phase should have a larger bulk modulus and a smaller equilibrium volume. This condition guarantees a double volume collapse along compression, which is a necessity for a first-order reentrant transition. Other thermodynamic properties also show a discontinuous or quasi-discontinuous jump at the PPT points. The inset in Fig. 4 draws the relative variation of thermal expansivity α with respect to its initial value along the 300 K compression curve. It deviates from the trend of the initial phase (as the dashed line shows) at point A and plunges to a new value, but at point B it jumps back to the previous curve, a key feature of the reentrant transition. Other physical quantities, such as specific heat and compressibility, demonstrate similar characteristics.

2. Coexistence of defects

The picture of pseudo phase of defects is only valid when the dominating region of the associated defect type is well defined. For point defects at low temperature, it is usually the case. However, with elevated temperature and/or when complex defect clustering is involved, competition might lead to coexistence of different defect species, where the notation of pseudo phase could lose its physical importance.

For realistic UO_2, pseudo phase can always be defined, whether oxygen clusters (e.g., the COT-o cluster) are involved or not. At high temperatures, the zone of the pseudo phase boundary becomes wide, and renders the PPT as a smooth crossover.[15] In spite of this, the material behavior still can be understood within the framework of pseudo phase. In some conditions, however, a situation that one defect species appears but never gains the dominant role might be possible. This will completely invalidate the picture of pseudo phase, and a detailed analysis of defect concentrations becomes necessary (in contrast to this, the defect concentrations are determined by stoichiometry deviation if pseudo phase can be applied).

An example of this is presented in Fig. 5, which was generated with JPC's formation energy data.[32] In addition to that, the value of the COT-o cluster[14] was also reduced by 4.865 eV; namely, we have artificially decreased the stability of oxygen clusters. The result is that oxygen interstitial O_i gets some promotion, but not enough to become the major one, and persists only within a narrow pressure range. It is evident from Fig. 5 that in this virtual system U_i and COT-o (at least for most pressure ranges) can be depicted using pseudo phase, and there is a PPT from U_i to COT-o at a pressure of 7 GPa. On the other hand, O_i, which appears from 20 to 50 GPa, depletes the concentration of COT-o slightly. But it never gains dominance, and the phenomenon must be taken as a defect coexistence rather than being a PPT. To understand the difference between these is crucial for a correct description of defective materials using the concept of pseudo phase.

IV. DEFECT INTERACTIONS

The above discussion is based on the approximation of PDM, which is valid at the dilute limit. With an increase of defect concentrations, however, interaction between defects becomes significant. This could lead to a severe deviation from the prediction of PDM. On the other hand, non-stoichiometry might affect the EOS and energetics of defects, thus modify the PPD. To obtain the correct defect behavior near the stoichiometry, a close cooperation between experimental measurements and theoretical analysis is necessary. For that purpose, a thorough and comprehensive understanding of defect interaction is crucial. This is because with such accurate information, we can deduce the formation energy at the dilute limit from the measured PPD at finite stoichiometry deviations. It is worth mentioning that the same extraction procedure can be done using the simple PDM, but the resultant error is usually quite large. In this part of the paper, we will first derive a general formalism that includes defect interactions, and then we will show that the conventional PDM can be adapted to take these interactions into account effectively with a simple

constant mean-field approximation, which greatly expands the applicability of the PDM.

A. General formalism

If one is interested mainly in macroscopic properties of a defective material averaged over a long enough time scale, the most important contribution comes from defects in static distributions. For a classical crystal at finite temperature, defects have nonzero probability of migrating between available sites. This alters the dynamics and transport property of the system. Nevertheless, diffusion does not modify the overall macroscopic properties very much as long as the distribution of defects is still in an equilibrium state. This is because migration is a transient process and most of the time defects are trapped in their equilibrium sites. In a migration process, defects induce dynamic deformations in the local lattice, and scatter with phonons. This effect might drive phonons away from equilibrium distribution. However, considering that this change is very small compared to thermal fluctuations and our interested time scale is many orders longer than the phonon relaxation time, it is justified to ignore this effect.

The main assumptions in the theory include the following: (a) We work on a lattice model, (b) only static distribution of defects is considered, (c) the distribution must be homogeneous, (d) dynamic effects due to defect migration are ignored, (e) no defect creation and annihilation are considered, and (f) when defect clusters are involved, taking them as single objects, namely, ignoring association and/or dissociation effects.

With these assumptions, let us consider a grand-canonical ensemble on a lattice in which the number of particles fluctuates around the average value. Assume there are in total K sublattices, which are occupied by M species of particles. Using N_i^m denotes the number of the mth kind of particle that is siting on the ith sublattice, where i can take any value from 1 to K and m varies from 1 to M. It is evident that each system in the ensemble is characterized by the occupation of particles on the lattice, and thus the ensemble can be grouped according to $\{N_i^m\}$. That is to say, each system can be labeled uniquely by a set of $\{N_i^m\}$ together with an auxiliary index s, where s runs over all possible configurations that has the same $\{N_i^m\}$. In this way, if using ρ_q denotes the probability of configuration $(\{N_i^m\},s)$ in the ensemble, where $(\{N_i^m\},s)$ has been shortened as q for brevity, then the Gibbs free energy of the ensemble is

$$G = \sum_q [\rho_q F_q + k_B T \rho_q \ln(\rho_q)]. \tag{18}$$

Here F is the Gibbs free energy of an individual configuration, and the contribution of configurational entropy has been separated out and presents as the second term in Eq. (18). The thermodynamically equilibrium state is achieved when G takes a minimum. The normalization condition requires $\sum_q \rho_q = 1$. If N^m denotes the total number of the mth particle in the ensemble, then $N^m = \sum_i \sum_q N_i^m \rho_q$. Introducing Lagrange multipliers μ_m and λ, the minimization equation of G becomes

$$\frac{\delta G}{\delta \rho_q} + \sum_m \mu_m \frac{\delta\left(N^m - \sum_i \sum_q N_i^m \rho_q\right)}{\delta \rho_q} + \lambda \frac{\delta\left(1 - \sum_q \rho_q\right)}{\delta \rho_q} = 0. \tag{19}$$

Making use of Eq. (18), this leads to

$$\rho_q = \exp\left(\frac{-F_q + \sum_i \mu_m N_i^m}{k_B T}\right) \Big/ \Xi, \tag{20}$$

where the partition function $\Xi = \sum_q \exp(\frac{-F_q + \sum_i \mu_m N_i^m}{k_B T})$. It can be shown that μ_m is just the chemical potential of the mth type of particle. The free energy of the qth configuration, F_q, which consists of the cold crystal energy at 0 K and phonon contributions to the internal energy and entropy (as well as a term of PV, if at finite pressure), can be calculated with modern first-principles methods. Since defects in an individual configuration manifest as an imperfect occupation of the lattice sites, the equilibrium thermodynamics of defects is therefore completely described by Eq.(20), in which the contribution of defect interactions arises from F_q.

When the energy scale of temperature is much smaller than the formation energy of defects, which usually is the case for most applications, the partition function is dominated by the perfect occupation (i.e., the ground state), namely $\Xi \simeq \exp(\frac{-F_0 + \sum_i \mu_m N_{0_i}^m}{k_B T})$, where the subscript 0 denotes the ground state. In this situation Eq. (20) reduces to

$$\rho_q = \exp\left(-\frac{\Delta G}{k_B T}\right), \tag{21}$$

where the FGE of configuration q is given by $\Delta G = F_q - F_0 + \sum_i \mu_m (N_i^m - N_{0_i}^m) = \Delta F + \sum_i \mu_m \Delta N_i^m$. For a single point defect $\Delta N = \pm 1$. Thus the FGE of intrinsic defects such as Frenkel pairs and Schottky defects can be derived straightforwardly from Eq. (21), and has the same form as Eqs. (5) and (6). Furthermore, equations similar to PDM [Eqs. (7)–(9)] also can be constructed easily using Eq. (21), indicating that the simple formalism of the PDM is much more flexible than what was originally proposed.

It is necessary to point out that for a system defined on a lattice, there is an orthogonal and complete basis set called correlation functions, which are an alternative but powerful representation of all possible occupation configurations of particles on the lattice using increasingly complex point sets ranging from a single point to nearest pairs and bigger clusters.[48] Any functions defined on the lattice can be expanded with such a basis. For defective crystals, the matrix and interstitial sites define such a lattice naturally. If we further introduce a special species of *white atom*, and regard all vacancies as those occupied by white atoms, then such orthogonal and complete correlation functions ξ can be defined. In this way, the probability for a configuration to appear becomes

$$\rho_q = \sum_j Y_{q,j} \xi_j, \tag{22}$$

and the Gibbs function of Eq. (18) can be rewritten as

$$G = \sum_j v_j \xi_j - T S_c, \tag{23}$$

with the configurational entropy given by $S_c = -k_B \sum_q [(\sum_j Y_{q,j} \xi_j) \ln(\sum_j Y_{q,j} \xi_j)]$, and the interaction strength of cluster $v_j = \sum_q F_q Y_{q,j}$. It is obvious that Eq. (23) has the same form as the theory for alloys.[49–51] Namely, both alloying and defects on a lattice can be described by the same unified theoretical framework. Within this method, the

interaction strength of clusters can be evaluated with cluster expansion method using *ab initio* total energy calculations,[52] and the configurational entropy may be evaluated by the cluster variation method.[53]

B. Effective point defect model

For a point defect on an infinitely large lattice (the dilute limit), the formalism discussed above naturally leads to the conventional PDM.[3,42] When defect concentration is finite but interaction between the defects is weak and can be ignored safely, the same conclusion holds. This is because for a configuration containing y noninteracting point defects, the corresponding FGE is just y times that of a single one, and then Eq. (21) gives rise to $\rho_{q_y} = (\rho_{q_1})^y$, which is exactly the result of PDM. Alternatively, for noninteracting defects, the presence of a defect has no influence on others, and we therefore can isolate a defect by cutting it and the associated local lattice out from the matrix, and then extend the surrounding lattice to an infinite range. This operation keeps the defective behavior. It maps noninteracting defects with finite concentrations onto a group of systems at the dilute limit, which justifies the application of the PDM.

When interactions between defects are substantial, it is almost impossible to isolate a defect from others. At a condition that the distribution of defects is homogeneous, however, we can approximate the interaction by a constant mean field. In this approximation, the defects and the associated local lattice environment that are cut out from the matrix keep the original size, and are subject to a field that takes a role of modeling the interactions with other homogeneously distributed defects that have been removed. To construct accurately an environmental field of such kind is difficult, if not impossible. For practical purpose, we may simplify it by using regularly distributed defects to simulate the field approximately. This sacrifices the rigidity of the theory, but makes the problem more tractable. What one needs to do now is to periodically repeat the piece of defective lattice that has been cut out from the matrix along the three-dimensional lattice vectors. In this way the periodical images of the defect take the role of modeling the homogeneous environment produced by other defects. Just one such configuration of course cannot capture the whole features of the defect interactions. By averaging over all possible regular defective distributions, nevertheless, one eventually can reach a converged result.

Generally the free energy of a system in the ensemble can be written as

$$F_q = F_0 + \sum_i A_i n_i + \frac{1}{2}\sum_{i,j} B_{ij} n_i n_j + \frac{1}{6}\sum_{i,j,k} C_{ijk} n_i n_j n_k + \cdots, \tag{24}$$

where n_i is the concentration of defect i in this system. If only up to linear terms are kept, then Eqs. (18) and (21) reduce back to the conventional PDM. The terms of higher order describe effective defect interactions, and should be important for any real materials with high defect density. On the other hand, if we know the values of parameter F_0, A, B, and C, the free energy (as a function of defect concentration n_i) of any defective configuration can be evaluated from Eq. (24) directly. To determine these parameters, one can solve Eq. (24) by a least-squares fit method using *ab initio* calculated F_q of a set of configurations. Furthermore, since the ΔG in Eq. (21) can be rewritten as

$$\Delta G = \Delta F^0 + \Delta F(n_i, n_j, \cdots) + \sum_i \mu_m \Delta N_i^m, \tag{25}$$

where the first term on the right-hand side represents the contribution of noninteracting defects, and the second term arises from defect interactions, Eq. (21) then leads to

$$\rho_q = \rho_q^0(n_i^0) \exp\left(-\frac{\Delta F}{k_B T}\right), \tag{26}$$

where ρ^0 is the probability predicted by the conventional PDM which gives a defect concentration of n^0 (determined by ΔF^0). For example, if there are d_i defects of the ith type appearing in the configuration q, where $n_i = d_i/D_i$ and D_i is the total available sites for that defect, PDM gives $\rho_q^0(n_i) = \prod_i (n_i)^{d_i}$. Because of the structure of ΔF as shown in Eqs. (24) and (25), ρ_q can be factorized into the same form as ρ_q^0. Namely,

$$\rho_q = \prod_i (n_i)^{d_i} = \rho_q^0(n_i). \tag{27}$$

We finally get

$$n_i = n_i^0 \exp\left[\frac{-1}{k_B T D_i}\left(\frac{1}{2}\sum_j B_{ij} n_j + \frac{1}{6}\sum_{j,k} C_{ijk} n_j n_k + \cdots\right)\right]. \tag{28}$$

This explicitly demonstrates that the simple formalism of the PDM is still valid even when defect interactions are present, as long as the defect distribution is homogeneous. The effect of interaction is to modify the defect concentrations in a constant mean-field way (here *constant* means that the interaction has been averaged over the whole configurational space so that no dependence on the distance between defects presents explicitly), and the formation energy of a single point defect Δf_i has to be changed from its dilute limit value Δf_i^0 to

$$\Delta f_i^0 \to \Delta f_i = \Delta f_i^0 + \frac{1}{2D_i}\sum_j B_{ij} n_j + \frac{1}{6D_i}\sum_{j,k} C_{ijk} n_j n_k + \cdots, \tag{29}$$

and the defect concentration equations also become

$$n_i^0 = \exp\left(-\frac{\Delta f_i^0}{k_B T}\right) \to n_i = \exp\left(-\frac{\Delta f_i}{k_B T}\right). \tag{30}$$

C. Behavior near the stoichiometry

In practice, one usually has to employ a finite size cell with periodic boundary conditions to simulate the defective structures. The formation energy and defect concentrations thus obtained in most cases do not correspond to the dilute limit. Making use of the effective PDM generalized in the above subsections, we can quantify not only how the interactions modify defect concentrations, but also the variation of defect formation energy as a function of defect concentrations, thus

TABLE I. First-principles results for the energy curve of $UO_{2\pm x}$, where x is the deviation from the stoichiometric composition of uranium dioxide. N is the total number of atoms in the simulation cell. D (in eV), r_0 (in Å), and B_0 (in GPa) are the cohesive energy per atom, the equilibrium lattice parameter of the effective cubic cell, and the zero pressure bulk modulus, respectively.

Structure	x	N	Functional	D	r_0	B_0	Phase
${}^{u}C1_1$	$-\frac{2}{5}$	13	LSDA + U	7.541	5.708	173.60	CaF_2(AFM)
$C1_{-1}$	$-\frac{1}{4}$	11	LSDA + U	8.002	5.443	189.32	CaF_2(AFM)
$C1_1$	$\frac{1}{4}$	13	LSDA + U	7.937	5.402	246.63	CaF_2(AFM)
${}^{u}C1_{-1}$	$\frac{2}{3}$	11	LSDA + U	7.616	5.284	114.59	CaF_2(AFM)
$C6_{-1}$	$-\frac{1}{24}$	71	LSDA + U	8.184	5.447	214.85	CaF_2(AFM)

providing a viable way to extrapolate defect energetics to the dilute limit. Taking UO_2 as a prototype, we will show in this part how interactions could alter defect behaviors.

According to Ref. 15 and the above discussions, pseudo phases in UO_2 are well defined: At most of the thermodynamic conditions in which we are interested, only one type of defect presents, and all other components are suppressed completely. This implies that only the diagonal terms in Eq. (24) make sense. Namely, only interactions between the same kind of defect need to be considered, which greatly reduces the number of *ab initio* calculations that are required for extraction of the interaction strengths B and C. Using configurations with different simulation cell size of $2 \times 2 \times 2$, $1 \times 2 \times 2$, and $1 \times 1 \times 1$ of the cubic fluorite unit, we extracted the defect interaction strength by solving a set of equations of Eq. (24). The employed energy curves for the smallest cell are listed in Table I (in which the defective structures are labeled following the same rule as in Ref. 14), and others are taken from Table I in Ref. 14. In particular, the results in Table I here were calculated using the VASP code, with the same LSDA + U setting as in Ref. 14. All structures were fully relaxed at a series of fixed volumes. Since the supercell size of these structures is relatively small, 36 irreducible k points were employed to ensure the total energy convergency.

With the effective PDM of Eq. (30), it is not necessary to work on the ensemble average of Eq. (18) any longer. Instead, the problem changes to "how the effectively independent defects distribute on the lattice." For the purpose of investigating the compression behavior of defects, it is helpful to employ a reference supercell, and normalize all involved energetics with respect to it. In doing so, however, the number of defects might no longer be an integer. A rescaling procedure is thus required when evaluating the formation energy of a *single* defect. Let Δe be the defect contribution in Eq. (24) that is evaluated in the reference cell, i.e., $\Delta e = F - F_0$, with a defect concentration n. The number of unit cells in a supercell which contains *one* and *only one* of this type of defect is $1/(nN_d)$, where N_d is the number of available sites for this defect in a unit cell. Then the energy difference for creating a defect is $\Delta E = \Delta e/(nN_dN_r)$, where N_r is the number of unit cells making up the reference supercell. In this way, the formation energy of a Frenkel pair for X species becomes

$$\Delta f_{\mathrm{X\_FP}} = \Delta E_{\mathrm{X}_v} + \Delta E_{\mathrm{X}_i}, \tag{31}$$

TABLE II. Formation energy (in eV) of intrinsic point defects in UO_2 of Frenkel pairs (O_FP and U_FP) and Schottky defect (Sch). $\Delta\overline{f}^0$ is the value approximated with a $2 \times 2 \times 2$ supercell, Δf^0 is the dilute limit value extrapolated using Eq. (29) up to cubic terms, and $\delta = \Delta\overline{f}^0 - \Delta f^0$.

Label	O_FP	U_FP	Sch
$\Delta\overline{f}^0$	5.38	14.34	10.53
Δf^0	4.77	13.78	10.21
δ	0.61	0.56	0.32

and the Schottky defect formation energy is

$$\Delta f_{\mathrm{S}} = 2\Delta E_{\mathrm{O}_v} + \Delta E_{\mathrm{U}_v} + \frac{3}{N}F_0. \tag{32}$$

Here N is the total number of atoms in a defect-free reference cell. For a $2 \times 2 \times 2$ supercell of fluorite UO_2, $N = 96$ and $N_r = 8$. Also for a cubic fluorite unit, N_d takes 8 for O_v, and 4 for O_i, U_v, and U_i, respectively. These formulations, together with Eq. (29), allow for extrapolating the intrinsic defect formation energy to the dilute limit by decreasing the defect concentration to an arbitrarily small value. The obtained results are summarized in Table II. We can see that a $2 \times 2 \times 2$ cell is not big enough to converge the formation energy to the dilute limit. The deviation from the extrapolated value is less than 1 eV. The largest one is the oxygen Frenkel pair in which δ reaches a value of 0.6 eV. It is at the same level as the finite-size correction of charged defects,[32] where a value of about 0.6 eV was also obtained for O_FP. This good agreement demonstrates that our treatment on defect interaction is at least qualitatively correct.

Inclusion of defect interactions in the PDM makes it possible to study the fine behavior over the whole stoichiometry. Figure 6 shows the relative variation of thermal expansivity α and compressibility χ as a function of stoichiometry deviation x at 300 K and 0 GPa, in which the solid points denote the exact value of the configurations that were employed to extract the interaction strength. It is evident that the linear approximation of Eq. (24) (namely the conventional PDM) fails to reveal the fine behavior of nonstoichiometric UO_2. Far from the point that was used to approximate the defect formation energy, it deviates from the exact value drastically. On the other hand, both quadratic and cubic approximations predict a curved variation of physical quantities correctly. It is interesting to note that the sharp tip appearing at the stoichiometry is very similar to the "W" shape anomaly in alloys.[43] Nevertheless, the underlying physics is different. Here it mainly originates from two facts: (a) the curvature due to defect interactions, and (b) the predominant defect types at the hyper- and hypostoichiometry sides are different, which gives rise to different variation trends of the physical quantities. From this perspective, measuring the departure of relevant physical quantities from a linear behavior near the stoichiometry would reveal the strength of defect interactions, and constrain the application range of the conventional PDM.

The above discussions reveal the power of including defect interaction into statistical mechanics models such as the PDM. Although by comparison with available experimental data one can assess the validity of our approach, due to the

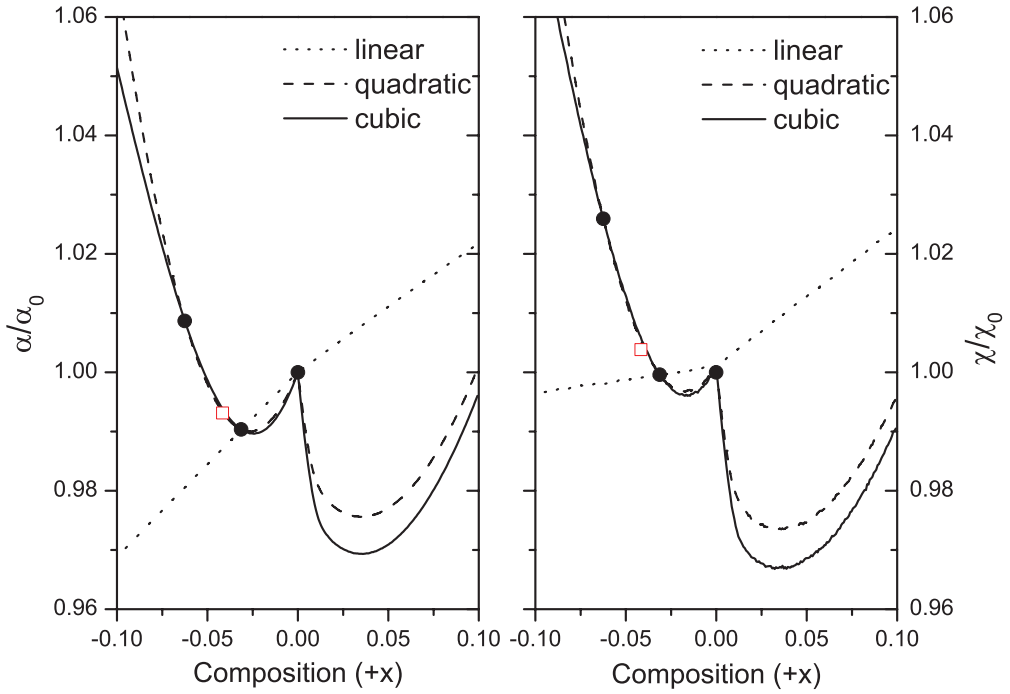

FIG. 6. (Color online) Relative variation of thermal expansivity (α) and compressibility (χ) with stoichiometry deviation x at different level of approximations. Notice the sharp tips at $x = 0$ due to defect interactions.

uncertainty of these data as mentioned in Secs. I and III, a quantitative validation has to be made with direct *ab initio* calculations. To this end, we made an independent calculation on a defective configuration of $C6_{-1}$, using a supercell of $1 \times 2 \times 3$ of the cubic fluorite unit, in which one oxygen atom has been removed to create one oxygen vacancy. The obtained energetics are listed in Table I, and the calculated thermal expansivity and compressibility are compared with that of effective PDM in Fig. 6 as the open square points. Note that in this separate calculation we employed only the experimental observation that the oxygen vacancy prevails in UO_{2-x}, and did not invoke any other approximations. Therefore the good agreement between these two results as shown in Fig. 6 provides a solid verification of the validity of our constant mean-field treatment of defect interactions for homogeneously distributed defects, as well as the effective PDM that is based on it.

V. DISCUSSION

A. Charged state

UO_2 is a semiconductor with a finite energy gap, it is possible that defects in it are charged rather than being neutral. Except for a very few studies,[29–32] most *ab initio* investigations on defective UO_2 assumed a neutral simulation cell, as we did here. In principle, such "neutral" calculations do not correspond to literally neutral defects, since local transfer of electrons might lead to a partial charge of the defects. Nevertheless, the finite size of the simulation cell imposes a constraint on the charge redistribution, and thus the defect might not reach its full charge state. This problem becomes very severe when at the dilute limit or near the stoichiometry, where defects can be fully charged only by exchanging electrons with valence/conduction bands, which is a kind of global charge redistribution. For large stoichiometry deviation, however, defects interact with the matrix strongly, leading to deep defect levels which are near either the gap middle or hybridization with valence/conduction bands. In both cases a neutral defect could be expected because it is difficult to *ionize* the defect at low temperatures in the first case and no charged defect can be supported in the second one.

For oxygen clusters, Crocombette argued that charged state makes them unfavorable at the stoichiometry.[32] It is reasonable. Actually, "neutral" calculations also indicated that oxygen clusters have negligible concentrations when near the stoichiometry.[21,22] Putting this information together, we ascertain that it should have no defect clustering when $x \approx 0$. But this does not mean that oxygen clustering is negligible at nonstoichiometry. The experimental evidence for such clustering was in fact observed at large values of x,[54–56] which is compatible with recent neutral calculations that predicted prevailing COT-*o* clusters at the hyperstoichiometry region. On the other hand, *ab initio* electronic structure revealed that the defect levels of the COT-*o* cluster hybridize strongly with the valence band of the matrix,[36] which implies that the cluster might be "neutral," or at least that these "neutral" results should partially reflect some physical reality. In these considerations, Crocombette's conclusion about charged oxygen defects[32] might lose the relevance when far from the stoichiometry. But overall the charged state of defects in UO_2 is still an open issue.

In the derivation of the general formalism of defects in Sec. IV, we did not consider the charged state. To include this is straightforward. One just needs to add an additional index to each type of defect to mark its charge state, and include

the chemical potential of free electrons to take the charge contribution at the Fermi level into account. Equation (18) then becomes

$$G = \sum_{q,Q}[\rho_{q,Q}(F_{q,Q} + Q\epsilon_f) + k_B T \rho_{q,Q} \ln(\rho_{q,Q})], \quad (33)$$

where Q is the total charge of the system, and ϵ_f the Fermi level. From this expression, the effective PDM which includes both defect interactions and variable charge state of defects can be derived easily.

B. Detection of PPT

Although PPT and the corresponding boundaries can be employed to constrain/extract the dilute limit of defect formation energy—an important quantity for understanding the stoichiometric behavior—to measure these boundaries is not a trivial work. At large stoichiometric deviation, the volume change at PPT is prominent, and thus it can be detected by measuring the quasi-discontinuous jumps in the EOS of defects.[15] Figure 7 plots a compression curve of $UO_{2+0.15}$ along a Hugoniot shocked from 300 K and 0 GPa. The volume collapse due to PPT from U_v to O_i (here we ignored oxygen clustering) is evident and therefore detectable. On the other hand, this pseudo transition pressure depends sensitively on the formation energy of O_i: It spans over a wide range of 40 GPa when there is a change in Δf_{O_i} about 4.0 eV. This property guarantees a good precision for the constraints on defect energetics.

At small value of x, however, the volume jump would be too weak to be perceptible. This is usually the case when $|x| < 0.02$.[15] In these cases, we cannot locate the PPT via measuring thermodynamic or mechanical quantities. However, since PPT changes the predominant defect species and thus the position of the defect level within the energy gap, transport properties are also modified. We therefore can detect the occurring of a PPT by measuring the sudden changes in electrical conductivity (or optical properties).[5] This method has high sensitivity that allows us to access the vicinity of the stoichiometry.

C. Instantaneous response

In the above discussions and also in Ref. 15, we froze the defect concentrations when evaluating the thermodynamic quantities. It is a theoretical requirement for the first derivatives of the Gibbs function, such as volume and entropy. But for higher order derivatives of the Gibbs function, it has no reason to do so because they are also defined by thermodynamic relations. In practice, however, a justification for this operation can be made. This is because for a classical crystal, the change of defect species can proceed via only atomic diffusion, which is a very slow process, and thus no defect can respond to rapid thermal fluctuations.

Then an interesting question arises, which is, what if defects can instantaneously respond to any disturbances? Simple analysis shows it might be fantastic. At first the magnitude of anomalies due to PPT would be amplified greatly, thus easing the difficulty in PPT detections. Figure 8 demonstrates this effect on the thermal expansivity α, bulk sound velocity, and specific heat at constant pressure C_P. The influence can be fully comprehended by comparing with Fig. 2 in Ref. 15, where defect concentrations were fixed when evaluating these quantities. Second, the compressibility would diverge at zero temperature. Considering the relationship between sound velocity and the compressibility, this implies a vanishing sound velocity (and the bulk modulus) in the vicinity of a PPT at low temperatures if defects have instantaneous response. On the phonon spectrum, it would manifest as an abnormal softening in acoustic branches at long wavelength (i.e., Γ point in the reciprocal space). This observation is tantalizing. But can it be true? We cannot answer it yet. Classical atomic diffusion of course cannot lead to a rapid response. But what if for a quantum crystal? In a quantum world particles are described by a wave function. If the wave functions of all defects are in a coherent state, then an instantaneous and simultaneous change

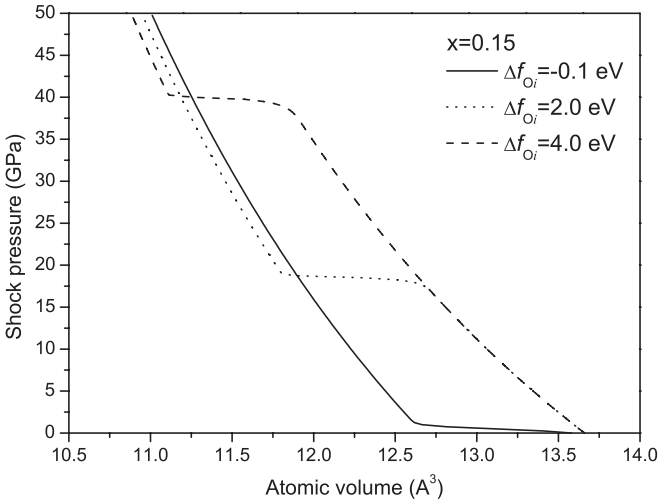

FIG. 7. Dependence of pseudo transition pressure from uranium vacancy to oxygen interstitial along a shock Hugoniot on the change of formation energy of oxygen interstitial. The stoichiometry deviation is $x = 0.15$.

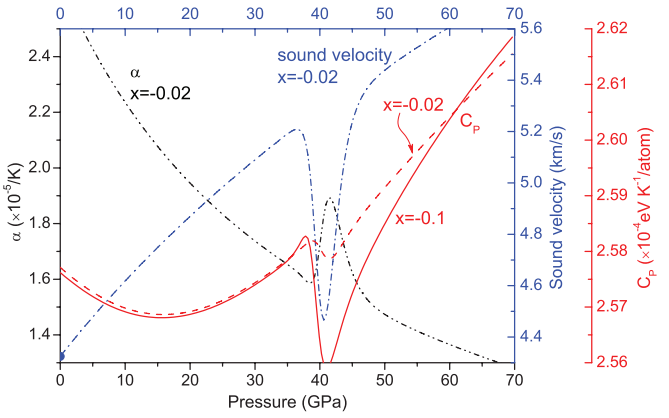

FIG. 8. (Color online) Anomalies in the thermal expansivity (α), isothermal bulk sound velocity, and specific heat at constant pressure (C_P) along a Hugoniot that shocked from 500 K and 0 GPa in nonstoichiometric UO_2 when defect concentrations have an instantaneous response to thermal fluctuations. The solid circle (at the bottom left corner) marks the experimental bulk sound velocity measured at ambient conditions in perfect UO_2.

of the defect species might be possible.[57] In this mechanism the requirement for a large-scale atomic diffusion has been removed, and a single change in defecton state is enough for a quantum pseudo transition to occur. Nevertheless, more theoretical works are necessary in order to pin down this possibility definitely.

VI. CONCLUSION

A general formalism for the thermodynamics of defects in a crystal was derived based on the statistics of a grand-canonical ensemble on a lattice. By introducing idle white atoms for vacancy and extending the sublattice of interstitial sites, this formalism has the same form as the lattice theory for alloys and compounds—a reflection of the unified physics underlying these seemingly different systems. With an approximation of constant mean field, this theory reduces to an effective point defect model in which defect interactions are included by an auxiliary field, whereas individual defects are treated as independent. In this way, we mapped a *many-body* defect system onto a *single* defect system by coupling it with an effective external field. If ignoring this field, the conventional PDM is recovered. This generalization greatly expands the applicability of the simple PDM. In order to explore the full content in this theory, we also studied possible reentrant PPT and multiple-defect coexistence with virtual systems.

Using PDM, we investigated the possibility of constraining defect energetics by measuring pseudo phase boundaries. By calculating the possible PPT between interested defects, we showed that the experimental estimates available in the literature, as well as a variety theoretical assessments, on defective energetics of UO_2 are not fully consistent. On the other hand, the range of energetics constrained by the PPTs overlaps with these estimates largely, and therefore has a potential to reduce the inconsistency in these data. By including defect interactions into the PDM, we demonstrated that the information obtained at finite stoichiometry deviation can be extrapolated to the dilute limit. Finally, we investigated the fine behavior of thermal expansivity and compressibility in the vicinity of the stoichiometry of defective UO_2, and some relevant issues of charged defects, detection of PPT, and possible instantaneous response of defectons in a quantum crystal are briefly discussed, in which we highlighted the detection of PPT by measuring electrical conductivity when near the stoichiometry, and the complexity arising from possible charged state of defects. Through these investigations, we clearly demonstrated that it is valuable to explore the whole nonstoichiometric range in order to acquire a comprehensive understanding about a defective material thoroughly.

ACKNOWLEDGMENTS

The authors acknowledge financial support from the National Natural Science Foundation of China under Grant No. 11274281, and Research Project No. 2012A0101001 supported by CAEP.

[1] F. Agullo-Lopez, C. R. A. Catlow, and P. D. Townsend, *Point Defects in Materials* (Academic Press, London, 1988).
[2] O. T. Sørensen, *Non-Stoichiometric Oxides* (Academic, New York, 1981).
[3] Hj. Matzke, J. Chem. Soc., Faraday Trans. 2 **83**, 1121 (1987).
[4] G. E. Murch and C. R. A. Catlow, J. Chem. Soc., Faraday Trans. 2 **83**, 1157 (1987).
[5] T. G. Stratton and H. L. Tuller, J. Chem. Soc., Faraday Trans. 2 **83**, 1143 (1987).
[6] R. Tetot and P. Gerdanian, J. Phys. Chem. Solids **46**, 1131 (1985).
[7] K. Clausen, W. Hayes, J. E. Macdonald, R. Osborn, and M. T. Hutchings, Phys. Rev. Lett. **52**, 1238 (1984).
[8] J. P. Crocombette, F. Jollet, T. N. Le, and T. Petit, Phys. Rev. B **64**, 104107 (2001).
[9] L. Petit, A. Svane, Z. Szotek, W. M. Temmerman, and G. M. Stocks, Phys. Rev. B **81**, 045108 (2010).
[10] S. L. Dudarev, G. A. Botton, S. Y. Savrasov, Z. Szotek, W. M. Temmerman, and A. P. Sutton, Phys. Status Solidi A **166**, 429 (1998).
[11] I. D. Prodan, G. E. Scuseria, and R. L. Martin, Phys. Rev. B **73**, 045104 (2006); **76**, 033101 (2007).
[12] H. X. Song, H. Y. Geng, and Q. Wu, Phys. Rev. B **85**, 064110 (2012).
[13] H. Y. Geng, Y. Chen, Y. Kaneta, and M. Kinoshita, Phys. Rev. B **75**, 054111 (2007).
[14] H. Y. Geng, H. X. Song, K. Jin, S. K. Xiang, and Q. Wu, Phys. Rev. B **84**, 174115 (2011).
[15] H. Y. Geng, H. X. Song, and Q. Wu, Phys. Rev. B **85**, 144111 (2012).
[16] F. Gupta, A. Pasturel, and G. Brillant, Phys. Rev. B **81**, 014110 (2010).
[17] D. A. Andersson, T. Watanabe, C. Deo, and B. P. Uberuaga, Phys. Rev. B **80**, 060101(R) (2009).
[18] D. A. Andersson, F. J. Espinosa-Faller, B. P. Uberuaga, and S. D. Conradson, J. Chem. Phys. **136**, 234702 (2012).
[19] D. A. Andersson, J. Lezama, B. P. Uberuaga, C. Deo, and S. D. Conradson, Phys. Rev. B **79**, 024110 (2009).
[20] H. Y. Geng, Y. Chen, Y. Kaneta, M. Iwasawa, T. Ohnuma, and M. Kinoshita, Phys. Rev. B **77**, 104120 (2008).
[21] H. Y. Geng, Y. Chen, Y. Kaneta, and M. Kinoshita, Phys. Rev. B **77**, 180101(R) (2008).
[22] H. Y. Geng, Y. Chen, Y. Kaneta, and M. Kinoshita, Appl. Phys. Lett. **93**, 201903 (2008).
[23] M. Freyss, T. Petit, and J. P. Crocombette, J. Nucl. Mater. **347**, 44 (2005).
[24] M. Iwasawa, Y. Chen, Y. Kaneta, T. Ohnuma, H. Y. Geng, and M. Kinoshita, Mater. Trans. **47**, 2651 (2006).
[25] B. Dorado, G. Jomard, M. Freyss, and M. Bertolus, Phys. Rev. B **82**, 035114 (2010).
[26] J. Yu, R. Devanathan, and W. J. Weber, J. Phys.: Condens. Matter **21**, 435401 (2009).
[27] F. Gupta, G. Brillant, and A. Pasturel, Philos. Mag. **87**, 2561 (2007).
[28] G. Brillant and A. Pasturel, Phys. Rev. B **77**, 184110 (2008).

[29]D. A. Andersson, B. P. Uberuaga, P. V. Nerikar, C. Unal, and C. R. Stanek, Phys. Rev. B **84**, 054105 (2011).
[30]P. Nerikar, T. Watanabe, J. S. Tulenko, S. R. Phillpot, and S. B. Sinnott, J. Nucl. Mater. **384**, 61 (2009).
[31]J. P. Crocombette, D. Torumba, and A. Chartier, Phys. Rev. B **83**, 184107 (2011).
[32]J. P. Crocombette, Phys. Rev. B **85**, 144101 (2012).
[33]P. Larson, W. R. L. Lambrecht, A. Chantis, and M. van Schilfgaarde, Phys. Rev. B **75**, 045114 (2007).
[34]G. Jomard, B. Amadon, F. Bottin, and M. Torrent, Phys. Rev. B **78**, 075125 (2008).
[35]B. Dorado, B. Amadon, M. Freyss, and M. Bertolus, Phys. Rev. B **79**, 235125 (2009).
[36]H. Y. Geng, Y. Chen, Y. Kaneta, M. Kinoshita, and Q. Wu, Phys. Rev. B **82**, 094106 (2010).
[37]V. I. Anisimov, J. Zaanen, and O. K. Andersen, Phys. Rev. B **44**, 943 (1991).
[38]A. I. Liechtenstein, V. I. Anisimov, and J. Zaanen, Phys. Rev. B **52**, R5467 (1995).
[39]S. L. Dudarev, G. A. Botton, S. Y. Savrasov, C. J. Humphreys, and A. P. Sutton, Phys. Rev. B **57**, 1505 (1998).
[40]F. Zhou and V. Ozolins, Phys. Rev. B **80**, 125127 (2009).
[41]F. Zhou and V. Ozolins, Phys. Rev. B **83**, 085106 (2011).
[42]A. B. Lidiard, J. Nucl. Mater. **19**, 106 (1966).
[43]H. Y. Geng, M. H. F. Sluiter, and N. X. Chen, Phys. Rev. B **72**, 014204 (2005).
[44]V. L. Moruzzi, J. F. Janak, and K. Schwarz, Phys. Rev. B **37**, 790 (1988).
[45]H. Serizawa, Y. Arai, M. Takano, and Y. Suzuki, J. Alloys Compd. **282**, 17 (1999).
[46]H. Serizawa, Y. Arai, and Y. Suzuki, J. Nucl. Mater. **280**, 99 (2000).
[47]M. Idiri, T. Le Bihan, S. Heathman, and J. Rebizant, Phys. Rev. B **70**, 014113 (2004).
[48]J. M. Sanchez, F. Ducastelle, and D. Gratias, Physica A **128**, 334 (1984).
[49]H. Y. Geng, N. X. Chen, and M. H. F. Sluiter, Phys. Rev. B **71**, 012105 (2005).
[50]M. Sluiter, D. de Fontaine, X. Q. Guo, R. Podloucky, and A. J. Freeman, Phys. Rev. B **42**, 10460 (1990).
[51]M. H. F. Sluiter, Y. Watanabe, D. de Fontaine, and Y. Kawazoe, Phys. Rev. B **53**, 6137 (1996).
[52]J. W. D. Connolly and A. R. Williams, Phys. Rev. B **27**, 5169 (1983).
[53]R. Kikuchi, Phys. Rev. **81**, 988 (1951).
[54]B. T. M. Willis, Proc. Br. Ceram. Soc. **1**, 9 (1964).
[55]B. T. M. Willis, Acta Crystallogr. Sect. A **A34**, 88 (1978).
[56]A. D. Murray and B. T. M. Willis, J. Solid State Chem. **84**, 52 (1990).
[57]D. I. Pushkarov, *Quasiparticle Theory of Defects in Solids* (World Scientific, Singapore, 1991).